

Performance Evaluation of Micromechanical Binary Phase-only Holographic Optical Elements

David A. Winick Bruce E. Duerwer S. Palchaudhury Paul D. Franzon

Integrated Electronic Systems Laboratory
Department of Electrical and Computer Engineering
North Carolina State University
Box 7911 Raleigh, NC 27695
<http://www.ece.ncsu.edu/erl/>

Abstract — This paper presents some results of our development and test efforts in micromachine design for optical modulation. In this work, we have developed, using a readily available surface micromachine fabrication process (MUMPs), a series of arrayed micromirror elements. These element arrays form phase-mostly spatial light modulators (SLM's), similar to Texas Instruments' flexure beam micromirror device (FBMD) [1]. Characteristics that distinguish our elements from those of TI include: integrated support posts to stabilize the elements at points beyond pull-in potential, non-metallic supporting structures to reduce diffractive noise, bistable drive capabilities without the need for transistor arrays, and greater mirror surface stability.

Sections 1 and 2 describe our elements (EmBMP's). Their arrayed operation is covered in Section 3. Optical evaluations in Section 4 measure the feasibility of these devices in the application of optical interconnect, as well as bracket further discussion concerning the use and technology requirements.

Key words: *holographic optical interconnect, spatial light modulators, digital micromirror devices.*

1 Introduction

The use of micro-electro-mechanically actuated elements for micromirror modulation of light has been successfully demonstrated by several parties [1] [2] [3]. However, despite the speed and cost advantages over optoelectronic solutions [4], their use in diffractive free-space optical beam routing has yet to gain acceptance. This is due to the size differential that still exists between MEMS and optical wavelengths. In order to use these devices in diffractive modulation, micromirrors must be optically stable, and their placement must at least approximate quarter-wavelengths. Additionally, space-bandwidth-products demand large arrays of tightly-spaced elements.

The element arrays discussed in this paper are operated

in digital mode, to approximate binary holographic elements, with applications in optical interconnect and projection display generation. The actuation characteristic of these elements, under proper biasing, exhibits a bistability that would enable low-power, high-yield elements that can be addressed progressively, in the form of a passive matrix. The ability to address an $N \times N$ array using $O(2N)$ lines from the periphery, rather than $O(N^2)$ lines or vertically-integrated logic, allows for relatively compact and inexpensive layout. A detailed explanation of this addressability is included in Section 3.

The design of these elements attempts to tackle several optical concerns, as well. The first of which is phase error. As flexible beams are actuated toward points of instability, deviations in thin-film amorphous material size, shape, and density would otherwise lead to deviations in mirror position. Most of the effects of these deviations are averted in our devices, which are driven beyond this region of instability. Stable states are kept as far from the pull-in condition as possible, in order to maintain stability.

2 Electro-mechanically Bistable MEMS Pistons

In this section, we discuss the design of electro-mechanically bistable MEMS pistons (herein referred to as EmBMP's) and their use as phase modulation elements. When arrayed, EmBMP's provide a compact, low-cost, low-power, and potentially efficient means for free-space optical modulation.

2.1 Theory of Operation

EmBMP's are micromirrors, fabricated in a micromachining process that provides a flat metal surface to reflect a free-space wavefront. The wavefront phase is modulated by mechanically re-positioning these micromirrors in the wavefront. The particular MEMS elements to which we

refer in this paper are termed ‘pistons’ after their up and down directions of movement.

EmBMP’s are controlled by mechanical placement of an upper capacitive plate relative to a lower plate, on the substrate. The plates are manufactured in an initial placement which reflects an ‘up’ position ($d = d_0$); as the plates are moved closer together, the capacitance increases, and a ‘down’ position is obtained ($d = d_0 - Gap_{stop}$). The element exhibits a strict two-position (‘up/down’) behavior due to a bistability in the electrostatic actuation that is used to move the plate.

Flexure beams used to support the upper plate act as springs. At least two must be used on each EmBMP for symmetrical stability; three can provide better stability in a hexagonal configuration, but keeping the beams long and of minimal count will reduce the necessary driving voltage. The electrostatic actuation (displacement) curve of the two capacitive plates follows an equation which is the sum of the capacitive actuating force and the returning (spring) force of the supporting flexure beams:

$$y(F) = \frac{F_{cap} L^3}{6NEI}$$

where F_{cap} is the force across two parallel plates of area A , gap distance $d = d_0 - y(F)$, and dielectric constant ϵ ; and the the other variables define the supportive structure:

$$F_{cap} = \sum_{cap} \frac{\epsilon V^2 A}{2d^2}$$

- L = beam length
- N = number of beams
- E = Young’s modulus
- I = inertial moment

Mechanical operation of the EmBMP occurs across a region of instability known as the “pull-in”. It is at this point that one of the two opposing forces overcomes the other. A mechanical stop is included to prevent the capacitive gap from closing completely; and an electrical bias is driven a marginal distance above the minimum-gap release voltage and below the pull-in voltage, to hold the switch in a stable position. From here, a small switching voltage can be used to open and close the switch.

Because the elements are capacitive in nature, they can easily store charge, with very little dissipation occurring only through the drive circuitry to maintain their positions. Furthermore, a slight modification of the previously explained drive method can take advantage of this (Figure 1 and Table 2.2), allowing large arrays of switches to be controlled via row and column strobe lines, as described in the next section. An advantage of this method is cost: these switches can be fabricated in a process that does not need transistors, and thus does not predicate corresponding dopant levels. A representation of the EmBMP’s

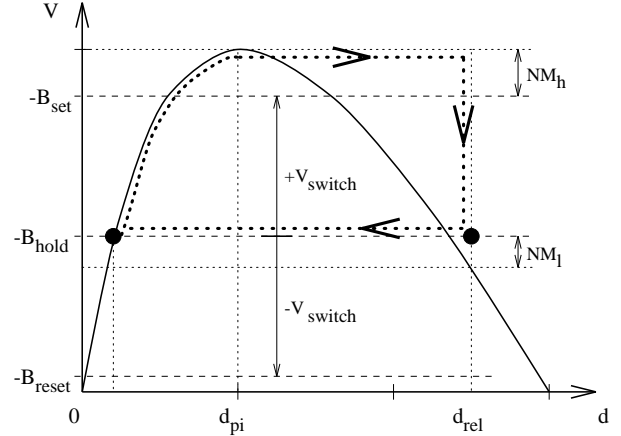


Figure 1: Electrostatic characteristic, voltage vs. displacement

movement between stable states is drawn over a portion of its characteristic curve below:

Since the mass and mechanical displacement is small, the switching speed of these devices is dependent on the pull-in voltage and mechanical settling time. An increase in switching voltage can vary the pull-in speed nearly linearly. The release speed, neglecting damping, is largely limited by the natural frequency, and therefore length, of the mirror-mass-coupled springs. Device speeds are expected to be in the 10’s to 100’s of kHz range, depending on structure and drive method. This pull-in and release speed are damped mainly by the ‘squeeze-film’ property [5] of air flowing between the two plates. In an array of such elements this flow is limited by the space between each element, and so is a function of mirror area coverage for the elements.

2.2 Fabrication

We have been researching these devices since the beginning of MCNC’s MUMPs process availability. They provide a mechanical device with the least amount of reliance on material quality or environmental wear-and-tear. The elevation of a very simple piston element design is shown below:

MCNC’s surface micro-machining is a process by which a structure of thin film materials layered on a substrate is subjected to a final fabrication stage that etches away any exposed sacrificial material. This final etch of chosen material results in movable mechanical structures. Mechanical actuation of these particular structures is then transduced from electrical energy sources (voltage) through the principle of electrostatics.

This process by which we created the elements discussed below consists of layers as described in [6]. The polysilicon layers, deposited via LPCVD, are Phosphorus doped and annealed for reduced internal stresses and fine grain

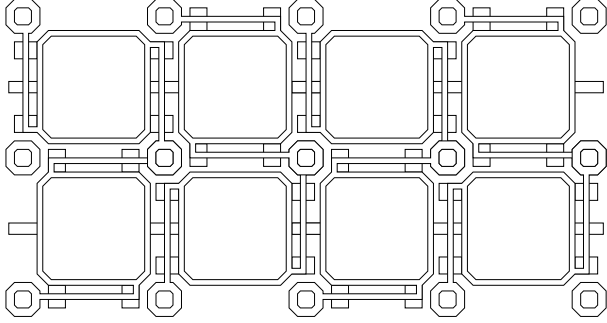


Figure 2: Typical piston array layout

size. Reactive ion etching (RIE) is used to pattern all of the layers, except the metal and nitride. The metal is patterned by lift-off. And the nitride layer acts to isolate the structure from the substrate, and is consequently un-patternable. The process also includes the ability to etch dimples, 7500Å deep, into the first layer of oxide. Use of this etch along with the calculated over-etch of other layer combinations allows us to build EmBMP's with many gap heights. These various gap heights result in the fabricated element designs which have characteristics shown in Figure 3 ('down' position gap heights for each curve are depicted by the horizontals of like line-type).

Selects (X_i, Y_j)	$+B_{reset}$	$+B_{hold}$	$+B_{set}$
$+V_{switch}$	hold	hold	set
$+0V$	reset	hold	hold

Table 1: EmBMP state control line voltages

2.3 Analysis and Outlook

The EmBMP drive capacitance must meet the following equation in order to fall beyond pull-in at minimum height (see characteristic curve):

$$(d_0 - Gap_{stop}) < \frac{2}{3}d_0$$

In simple geometries pull-in typically occurs after the top plate has moved 1/3 of its distance toward the bottom plate; the voltage at this point is V_{PI} . Following pull-in, the voltage across the plate must be reduced in order to return the top plate to an 'up' position; this release voltage is termed V_{rel} . A Gap_{stop} is built into each element to prevent the upper and lower plates from contacting.

For maximum stability (resistance to driver noise), a small $\frac{V_{rel}}{V_{PI}}$ ratio should be chosen, in order to maintain stability points at a steeper portion of the characteristic. Increasing the number of beams will increase angular stability, and thus maintain operation near this curve. Beam length and capacitive area can then be selected for appropriate drive levels and speed.

We have tested piston type 12M1D2 devices to reliably operate at pull-in and release voltages of 28.6V and 19.5V, respectively. Although fringing effected the actual capacitance of these devices (Figure 4 shows difference between Fastcap data and parallel plate model), these drive voltages correspond closely to the design $\frac{V_{rel}}{V_{PI}}$ ratio. Other device types have offered correspondingly similar responses, as well, with error likely due to film elasticity or thickness deviations.

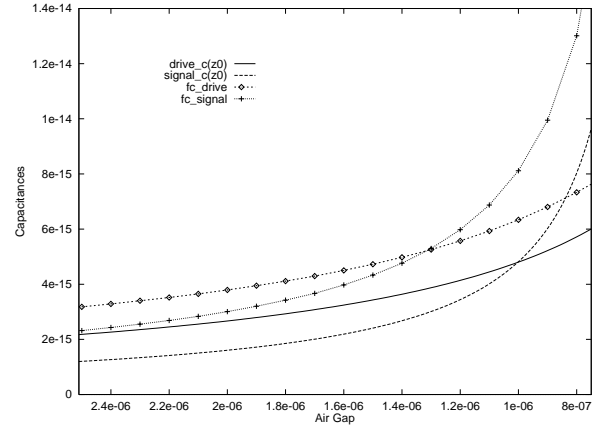


Figure 4: 3D data vs. parallel plate model

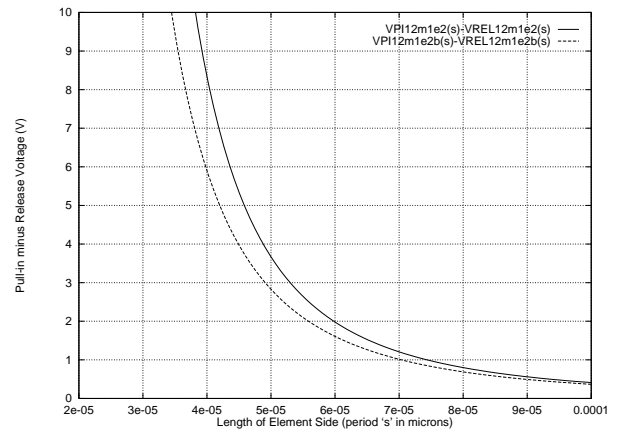


Figure 5: EmBMP switching voltage estimation

3 Arrays

The EmBMP's are arranged in a 2-dimensional array, where each element micromirror acts to reflect a chosen phase level of an incident beam, approximating a holographic optical element [7]. Both rectangular and hexagonal arrays have been designed, with center-to-center spacing periods no less than $42\mu m$, limited by feature size and design rule constraints. In order to conserve space, one direction of strobe lines connects to the lower electrodes using 0^{th} -layer polysilicon, while the other connects upper

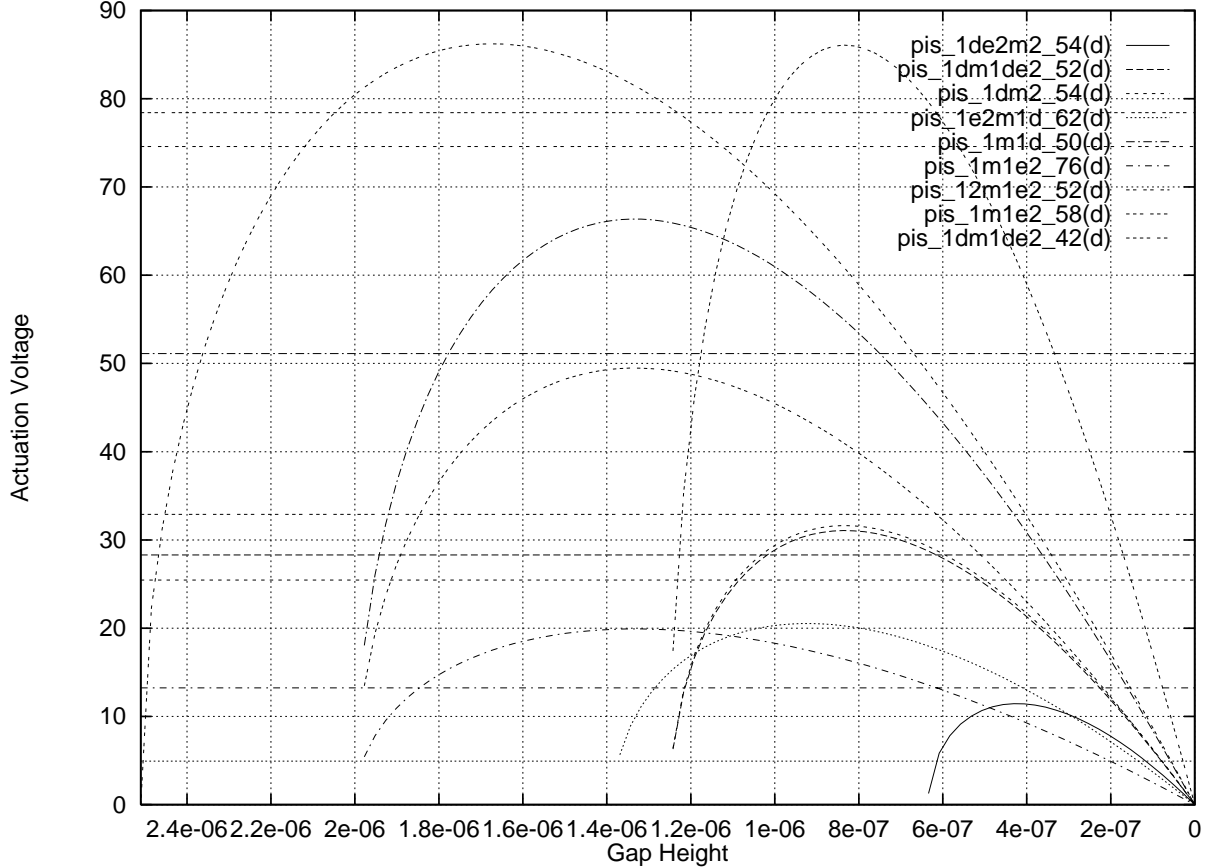


Figure 3: HC4 piston actuation characteristics

electrodes through the springs. By alternating element rotations (see Figure 2), it is possible to share anchors and extend springs across opposing sides of each element.

3.1 Programming the Elements

Programming of the array element positions is performed based on two sets of voltage levels reaching each element (see Table 2.2). Figure 1 shows how the voltage across each piston can be divided into a switching voltage, V_{switch} , and a bias voltage. $-B_{hold}$ is chosen just above the release level, $-B_{set}$ is chosen just below the pull-in level, and $+V_{switch}$ becomes the voltage in between. Thus when switching voltages ($+0$, $+V_{switch}$) are carried on row strobes and bias voltages ($-B_{set}$, $-B_{hold}$, $-B_{reset}$) are carried on column strobes, the array elements can be programmed row-by-row. In order to hold the programs of all the rows, $-B_{hold}$ should be maintained on each. To set (“down”) certain elements in a row, the corresponding row strobe should carry $-B_{set}$, and the column strobes for those elements should carry $+V_{set}$. Likewise, to reset (“up”) certain elements in a row, the corresponding row strobe should carry $-B_{reset}$, and the column strobes for those elements should carry $+0V$.

4 System Evaluation

Evaluation of EmBMP performance in this section is based upon its ability to modulate and incident optical wavefront as a programmable holographic optical element, for beam steering and focusing. The use of a mosaic structure, such as that found in EmBMP, for display generation exhibit several interesting modulation transfer function properties which are beyond the scope of this paper.

The mosaic structure is formed by pixelation in the EmBMP modulator. Each micromirror is spaced from its neighbor in order to provide freedom of movement. Unfortunately, this spacing causes some loss in incident power. Part of that loss is due to light hitting the spaces instead of the micromirrors. And part is due to a diffractive envelope function that is created by the effective aperture of each micromirror in the EmBMP spacing.

The micromirror coverage area of each element has drastic effects on optical efficiency. We have found that for an EmBMP array of 64×64 elements, a coverage of 88% (equal to that of TI’s commercial micromirrors) and size of twice the incident beamwidth is necessary to maintain less than 1dB loss simply due to light not reaching the micromirrors. While this array is possible with current

technology, it does pose some system topography limitations due to its size. One method of compensation, which we are currently investigating, is the use of diffractive microlenses, to give an effective 100% fill-factor to each micromirror.

4.1 Beamsteering

An EmBMP array can be modeled as an array of like apertures. Consequently the resulting wavefront is calculated as the convolution of the shape function, defined by the array program, and the envelope function, defined by micromirror coverage. This envelope function acts to reduce the efficiency of the system for larger beamsteering angles.

Another source of loss in beamsteering is the space-bandwidth product:

$$SBWP = (Bd)^2$$

where B is the highest programmable spatial frequency (and smallest increment, therefore, between each frequency), and d is the size of the array (and thus the number of increments that can be programmed). The SBWP describes the maximum theoretical number of target directions that can be independently specified. Since the size of EmBMP element is still relatively large compared to wavelength, a reduction in the number of programmable grating periods at small diffraction angles is apparent. Furthermore, since the binary nature of the EmBMP only allows two-phase programming, any diffraction will be symmetrical; consequently, the usable output plane must be divided in half, in both dimensions. Simulated output of a one-dimensional grating program, at maximum steering angle (Nyquist limit), is shown in Figure 6, for a 32×32 array of $10\mu m$ elements, and near-infrared wavelength. Loss can be attributed to both the negative order and higher orders. A partial solution to this problem, which we are also currently investigating, is the addition of a constant (quarter) phase to half of the array elements, in order to recover power from the negative diffraction orders.

4.2 Focusing

EmBMP arrays can also be programmed as a Fresnel lens. Figure 7 shows the phase program of an F/57 lens in a 32×32 array with 30% micromirror coverage, as we have fabbed in MUMPs. The resulting intensity profile, at focal length, is shown in Figure 8. When compared to that of an F/100 program (Figure 9, you can see that, like beamsteering, higher-order noise becomes apparent when approaching maximum programmable frequencies. Encoding schemes to optimize diffraction efficiency of the output, such as phase rotation, low-resolution encoding, and simulated annealing, are being investigated.

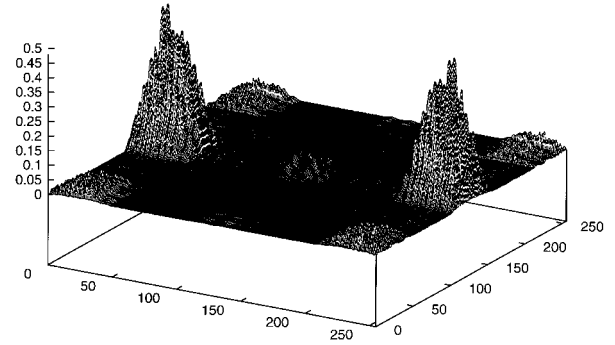


Figure 6: Simulated EmBMP beam steering capability

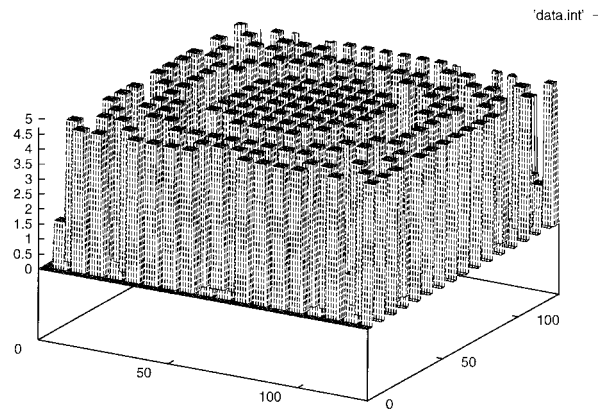


Figure 7: EmBMP phase program for F/57 lens

5 Conclusions

Flexure-beam actuators have been proven as high yield and high reliability MEMS devices, even in large arrays. Similar devices are already incorporated in commercial display products by Texas Instruments and airbag deployment mechanisms by Analog Devices. The compactness and long life of EmBMP devices, due to minimal wear, supplement their applicability as optical modulation mechanisms. With proper layout techniques and fabrication process, we feel these modulator arrays can be designed to fit between free-space optical beam paths, for beam steering, signal routing, and micro-adaptive optics.

Electro-mechanically bistable MEMS pistons can be built with low-cost materials, driven at relatively low operating power, and laid out in a reasonably small footprint for optical modulation. We are currently investigating their continued technology advancement and development for chip-to-chip optical data lines and airborne laser radar systems.

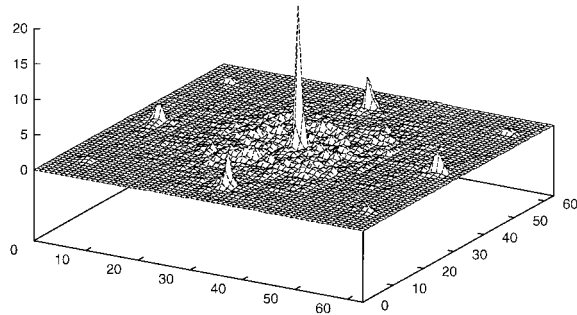


Figure 8: EmBMP output for F/57 program

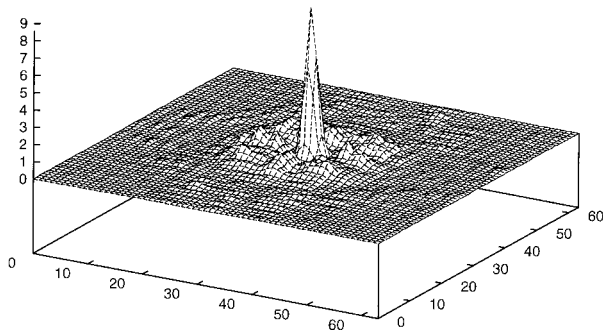


Figure 9: EmBMP output for F/100 program

- [3] Frank Merat and Mehran Mehregany, "Integrated micro-opto-mechanical systems", in *Micro-Optics/Micromechanics and Laser Scanning and Shaping*, M. Edward Motamedi and Leo Beiser, Eds., San Jose, CA, Feb. 1995, pp. 88–98.
- [4] D. C. O'Brien, R. J. Mears, T. D. Wildinson, and W. A. Crossland, "Dynamic holographic interconnects that use ferroelectric liquid-crystal spatial light modulators", *Applied Optics*, vol. 33, no. 14, pp. 2795–2803, May 1994.
- [5] Gary Keith Fedder, *Simulation of Microelectromechanical Systems*, Ph.D. dissertation, University of California at Berkeley, Sept. 1994.
- [6] Karen W. Markus and David A. Koester, *Multi-User MEMS Process (MUMPs) Introduction and Design Rules*, MCNC, Electronic Technologies Division, Mar. 1994.
- [7] David A. Winick, W. Michael Teague, and Paul D. Franzon, "A micro-machined approach to optical interconnect", in *45th Electronic Components and Technology Conference*, Caesars Palace, Las Vegas, Nevada, May 1995, Components, Hybrids, and Manufacturing Technology Society, IEEE, pp. 780–785.

Acknowledgments

This work is accomplished with much needed support, and the authors wish to thank the following funding sources: NSF for Dr. Franzon's Young Investigator's Award, Motorola and IEEE/CPMT for laser technologies and Mr. Winick's Fellowship, and DARPA/USAF for related contracts and grants. Also to the software developers for use of their tools: Cadence, Fastcap, and LightPipes.

References

- [1] Tsen-Hwang Lin, "Integration of micromirror and mixed-signal ics for optical information processing", in *Micro-optics/micromechanics and laser scanning and shaping*, San Jose, CA, Feb. 1996, SPIE – The International Society for Optical Engineering, pp. 78–87.
- [2] Gleb Vdovin, Simon Middelhoek, and Lina Sarro, "Spatial light modulator based on the control of the wavefront curvature", Tech. Rep., Laboratory of Electronic Instrumentation and DIMES, Delft University of Technology, The Netherlands, 1995.